

NIST Standard Reference Materials for Characterization of Instrument Performance

James P. Cline

National Institute of Standards and Technology, Gaithersburg, Maryland

1. INTRODUCTION

With a conventional powder diffractometer, practical data collection rates can be obtained from laboratory X-ray sources with the utilization of a divergent beam illuminating a flat powder specimen. Sample preparation is relatively simple and can be applied to a variety of materials. However, the para-focusing optics of these diffractometers embody aberrations from the ideal focusing geometry, rendering the performance characteristics, reflected by profile displacement, profile breadth, profile asymmetry, diffracted intensity as a function of 2θ angle, etc., to be a convolution of a number of contributing factors. To fully utilize the data from such equipment, the performance characteristics inherent to the diffractometer must be taken into account in the data analysis procedure. While the performance of such machines can be modeled, the more typical approach involves the use of standards for an analysis of instrument performance. The difficulties are compounded if the machines are set up incorrectly, as this results in additional aberrations, which are further convolved with those inherent to the para-focusing diffractometer. This results in a deterioration of the performance characteristics, which, while it may go undetected, affects the quality of the interpretation nonetheless. With the proper use of National Institute of Standards and Technology (NIST) standard reference materials (SRMs) the performance of equipment can be characterized accurately, allowing for the sources of error to be isolated and corrected.

2. PARAMETERS DEFINING INSTRUMENT PERFORMANCE AND NIST STANDARD REFERENCE MATERIALS

The five major aspects of a diffractometer's performance are: (1) position of profile maxima, or line positions, (2) profile shape, (3) overall intensity, (4) instrument response, or diffracted

intensity as a function of 2θ angle, and (5) single-to-noise ratio. The combination of the first two is generally referred to as the instrument profile function, (IPF). The ability of a material to serve as a standard depends on its microstructure and, to a lesser extent, on its crystallographic properties. The microstructure of an "ideal" standard, one that could serve for the complete characterization of an instrument, is certainly conceivable. However, realization of such an SRM is prohibited largely by difficulties in fabricating the desired material on the multi-kilogram scale required for SRM production. Thus, NIST provides several SRMs which can be used for diffractometer evaluation, each tailored for evaluation of a specific parameter. The user judges which performance criteria are most critical to the application and then selects the appropriate standard(s).

The primary profile position and shape parameters used for characterization of instrument performance are illustrated in Fig. 1. Unfortunately, what would appear to be one of the more straightforward parameters, the peak position, is described with any one of several conflicting definitions. The common one used by conventional X-ray powder diffraction community is the position in 2θ of maximum diffracted intensity, as shown in Fig. 1. Software packages are available for determining the position defined in this manner; however, results will vary depending on user input and the algorithm(s) used to analyze the data. The least computationally intensive methods are based on first- or second-derivative peak location algorithms that report the positions at the 2θ value where a local maximum in diffraction intensity was determined to exist in the raw data. Profile fitting with empirical shape functions affords greater accuracy and, when the code is specific to X-ray powder diffraction, will report the position as the intensity maximum of the $K_{\alpha 1}$ component only. The difference between the results from these two methods will be apparent at lower angles where the $K_{\alpha 1}$ and $K_{\alpha 2}$ components are not well resolved. Alternative descriptions of peak position include the seldom used peak centroid and the "corrected"

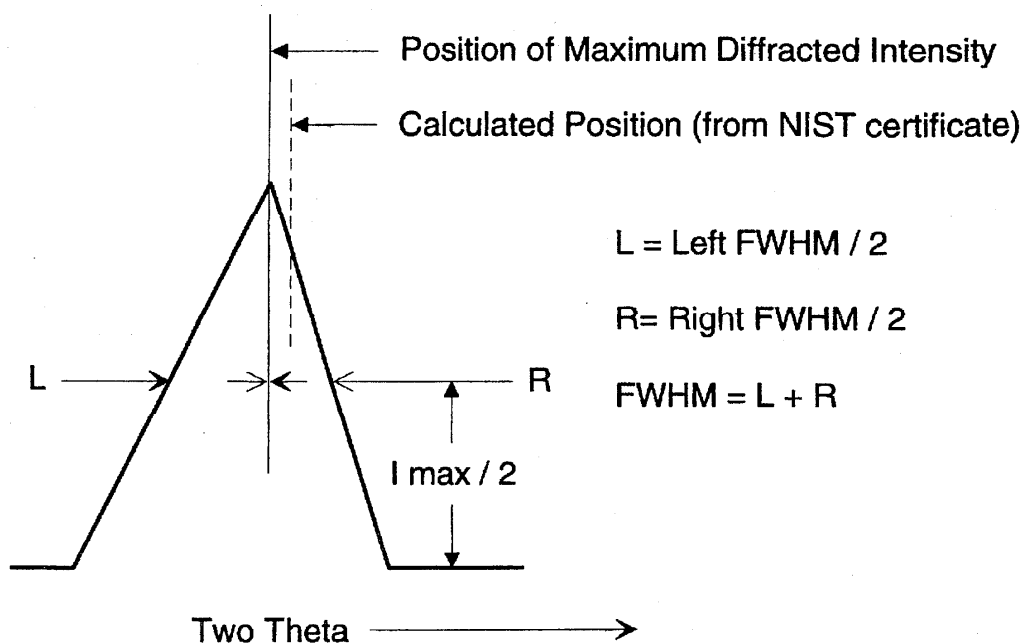


Figure 1 Diagrammatic illustration of profile position and shape parameters.

peak positions; the latter definition is discussed later. The "calculated position," shown in Figs. 1 and 2, is that obtained from the use of the NIST certified lattice parameter in a d -space computation. This computation also requires knowledge of the wavelength of the radiation. The difference between the "calculated" positions and the positions of maximum diffracted intensity, that is, $2\theta_{\text{calc}} - 2\theta_{\text{Imax}}$, plotted as a function of 2θ angle, yields a delta 2θ plot, an example of which is shown in Fig. 2.

The full width at half maximum (FWHM) is defined as the profile width at one half the value of maximum intensity after a background subtraction. When an asymmetric profile shape function is used in profile fitting, both left and right values of FWHM are reported. Such values are generally the full width of a symmetric peak, which corresponds to the shape of the right or left half of the refined profile. While data concerning peak position can be obtained via second-derivative-based algorithms, a full description of the IPF is obtained from profile fitting the observed data with a selected empirical function (such as Voigt, split Pearson 7, etc.). Plots of delta 2θ , FWHM, and the ratio of left to right FWHM versus 2θ angle yield a fairly complete graphical description of the IPF. However, plots of more detailed parameters defining profile shape are also of interest, that is, Pearson 7 exponents etc. The fitting of individual profiles results in data that are unconstrained to follow any functional dependence 2θ therefore, these data will reveal those defects in instrument performance that are localized to small angular regions in 2θ .

While "conventional" data analysis methods seek to parameterize the form of the raw data, a second category of more advanced methods seeks to characterize the nature of the experiment itself. Models are used that relate the form of the raw data to physical parameters pertaining to the microstructural and crystallographic aspects of the specimen and/or the optical aspects of the equipment. These models, in conjunction with a set of suitable physical parameters, are used to compute the corresponding powder diffraction

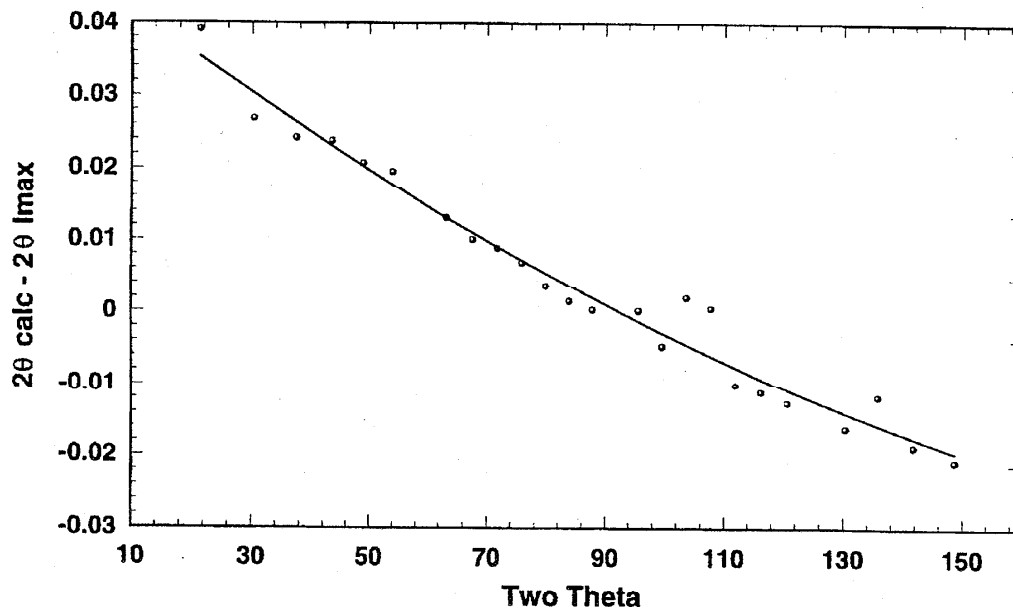


Figure 2 Delta two theta curve and second-order polynomial fit, for Siemens D500 with an IBM and PSD, determined with SRM 660, LaB₆.

pattern. The physical parameters are then varied in a least-squares refinement to obtain a best fit between the observed and calculated data. The models that address the optical aspects of the equipment are developed assuming that aberrations caused by the para-focusing geometry of the conventional powder diffractometer will influence the data in a specific manner. Improperly aligned equipment will exhibit deviations from these expected aberrations and thus will render the applicability of the models, and the refined parameters, to be of questionable validity.

The fundamental parameters approach (FPA) (Cheary & Coelho, 1992) can utilize single or multiple profiles in an analysis that relates the shape and position to the optical parameters, divergence slit size, source width, etc. of the conventional X-ray diffractometer. A somewhat less sophisticated alternative to the FPA, which can also be applied to the analysis of single profiles, consists of the Finger model (Finger et al., 1994) in conjunction with a Voigt profile shape function. The Finger model relates the degree of profile asymmetry to effects of axial divergence. The Rietveld method (Rietveld, 1969) uses the entire pattern for an analysis of the microstructural and crystallographic properties of the specimen; the equipment is described using analytical models or, more recently, by the FPA (Koalariet, at www.ccp14.ac.uk/tutorial/xfit.95/xfit.htm; BGMN, at www.mineral.tu-freiberg.de/mineralogie/bgm/index.html). Routines using physical profile functions, be they single profile or whole pattern, report the peak positions that result from the use of the model(s) in the code and are thus "corrected" for the expected aberrations affecting the raw data. These are often reported as "observed" reflection positions to differentiate them from the positions of the computed pattern. Obviously, if the models incorporated in such codes are valid, fully describing the optics, and the instrument is properly aligned, the data in Fig. 2 would form a horizontal line through zero.

The crystal structure obtained with the use of the Rietveld method serves as an effective and independently verifiable means to evaluate instrument performance. With the use of standards, one can verify that the range of refined parameters is plausible, validate instrument performance, and lend credibility to results obtained from unknowns. The evaluation of instrument response, or diffracted intensity as a function of 2θ , may be accomplished by conventional methods wherein peak intensities measured from the test instrument are compared with those of a standard. Using the Rietveld method, instrument response is evaluated in the context of intensity-sensitive parameters such as crystal structure and Lorentz-polarization (LP) factors. Consideration of the values obtained in the Rietveld analysis will offer the most effective means of discerning defects that vary smoothly over the full range of two-theta. However, errors within limited regions of 2θ , apparent in the data obtained from profile fitting, can be obscured in the case of a Rietveld analysis. A suitable standard for such an evaluation would possess a well-established crystallographic structure, exhibit a large number of lines (be of low crystallographic symmetry or have a large unit cell), and be of isometric crystal shape so as to not exhibit preferred orientation.

A list of NIST SRMs for powder diffraction is given in Table 1. Further information on NIST SRMs can be obtained at the NIST Technology Services web site: www.ts.nist.gov/srm. SRM 640c, an Si powder, is the primary line position SRM and is the SRM of choice in critical lattice parameter determinations. SRM 675, mica (fluorophlogopite), is certified with respect to lattice parameter but is primarily intended for calibrating 2θ at low angle. While SRM 660, an LaB_6 powder, is certified with respect to lattice parameter, its microstructure is such that it displays a minimum of line broadening that could be detected with conventional instrumentation. Thus, it is intended for characterization of the IPF. SRM 1976, a sintered alumina plate, is also certified with respect to lattice parameter, and since it also displays a minimal amount of profile broadening, it can

Table 1 NIST SRMs Certified for Powder Diffraction

SRM	Type	XRD application	Lattice parameters (nm)	Unit size (g)
640c	Silicon powder 2 θ /d-spacing	Line position		In preparation
656	Silicon nitride	Quantitative analysis	α -(0.7752630/0.5619372) β -(0.7602293/0.2906827)	10 10
660a	LaB ₆	Line profile		In preparation
674a	Powder diffraction intensity	Quantitative analysis		
	α -Al ₂ O ₃ (corundum)		(0.4759397/1.299237)	10
	CeO ₂ (fluorite)		(0.5411102)	10
	Cr ₂ O ₃ (corundum)		(0.4959610/1.358747)	10
	TiO ₂ (rutile)		(0.4593939/0.2958862)	10
	ZnO (wurtzite)		(0.3249074/0.5206535)	10
675	Mica	Line position, low 2 θ	0.998104	7.5
676	Alumina (corundum)	Quantitative analysis	0.475919/1.299183	20
1878a	Respirable quartz	Quantitative analysis		In preparation
1879a	Respirable cristobalite	Quantitative analysis		In preparation
1976	Alumina plate, sintered	Instrument response ^a	0.4758846/1.299306	4.5 cm×4.5 cm×0.16 cm

Note. Values in parentheses are not certified but are provided as reference values or are given for information only.

^a Formerly "instrument sensitivity."

also be used for characterization of the IPF. However, the overlapped lines it displays will lead to greater uncertainties in refined profile shape parameters, and the increased penetration of the incident beam due to its lower attenuation will result in larger profile breadths than those obtained with SRM 660. SRM 1976 was certified for calibration of instrument response through a comparison of observed and certified intensity values. Its sintered form eliminates the impact of sample mounting procedure on recorded diffraction intensities; it displays a moderate amount of texture. When the Rietveld method is to be used for evaluation of intensity factors, the high-purity, nonorienting (isometric), fine-grained alumina powder of SRM 676 renders it a suitable test material with respect to the requirements of such an analysis. Several additional SRMs, shown in Table 1, consist of high-purity, fine-grained powders intended for use as quantitative standards.

3. MEASUREMENTS AND ANALYTICAL PROCEDURES ADOPTED WITH NIST STANDARDS

Although a variety of methods and SRMs could be successfully employed for instrument characterization, at NIST we generally use SRMs 660 and 676 for this purpose. Initial evaluation of the equipment involves consideration of data obtained from profile fitting a scan of LaB₆; this is followed by a Rietveld analysis of data from both SRMs. The specimen of LaB₆ should be prepared so as to maximize the packing density and minimize the surface roughness. The specimen used at NIST consists of a disk of SRM 660 prepared by infiltrating a pressed compact of the powder with vacuum leak sealant. This results in a mechanically stable specimen that meets the aforementioned dual criteria of "ideal" specimen mounting.

Data are collected for the full range of 2θ with an overnight scan utilizing a step width that insures six points above the FWHM for all peaks. Data are then fitted with the split Pearson 7 profile shape function. Despite the lack of physical meaning associated with the refined parameters, the split Pearson 7 is preferred due to its superior capability in fitting the range of profile shapes observed in divergent beam powder diffraction. It is our intent to simply characterize the performance of the equipment through an accurate representation of the profile shapes.

The choice of software used for profile fitting will not affect the results, assuming that the selected package is working correctly. The Socabim (Siemens/Bruker)* program Profile was utilized for the data presented herein. The program Profile has two virtues that lend it to this application: (1) It can run in batch mode, utilizing command files to produce a complete set of refined data in a few seconds, and (2) it can output data in export formats for subsequent analysis by spreadsheet programs. The refined parameters are processed in Excel to compute such factors as $\Delta 2\theta$ and then is plotted via Stanford Graphics/Origin using previous files as templates. With this procedure we can generate the desired plots in a timely manner. Examples of these data from a Siemens D500 diffractometer equipped with a Johansson Ge (111) incident beam monochromator (IBM), combination sample spinner and changer, and a position-sensitive detector (PSD) are shown in Figs. 2 through 4.

Shown in Fig. 2 are the values of $\Delta 2\theta$, as a function of 2θ , along with a second-order polynomial fit to these data. The most common methods in which NIST line position SRMs are utilized, the "conventional" methods, involve the determination and polynomial fitting of a $\Delta 2\theta$ correction curve as illustrated in Fig. 2. The peak positions of this plot were determined via profile fitting, which, as has been stated, is more accurate than the derivative-based peak location algorithms. However, care should be taken to insure that the algorithm used to determine the peak positions of the standard is also the one used to evaluate those of the unknown. Otherwise, errors will be introduced. The coefficients determined via the polynomial fit are then used to correct the peak positions of subsequent unknowns for instrumental aberrations. This method cannot account for differences in placement and transparency between unknowns and standards; therefore, greater accuracy can be achieved when the standard is admixed with the unknown, with the data being corrected in an analogous manner. These two methods are termed the external and internal standard methods, respectively. In either case, corrected peak positions can then be used in a refinement for determination of lattice parameters. The use of the "conventional" internal standard method routinely yields results that are accurate to parts in 10^4 (Edmonds et al., 1989). It should be noted that these methods will correct for instrumental aberrations regardless of their form, that is, the form of the data in Fig. 2; they need only be continuous and not so ugly that they cannot be modeled with a low-order polynomial.

The data in Figs. 2 through 4 offer the most critical information in evaluation of diffractometer alignment and performance, and first should be examined for discontinuities and lack of smoothness. Unfortunately, the rigorous assignment of error bars to these data is difficult. The programs that generate the data may list estimates of the standard deviation (ESDs) associated with each refined parameter. The ESDs so listed are indicative of random variation due to counting statistics, which impart Poisson noise to the raw data, and rep-

* Certain commercial equipment and manufacturers are identified in order to specify the experimental procedure adequately and do not imply a recommendation or endorsement by the National Institute of Standards and Technology.

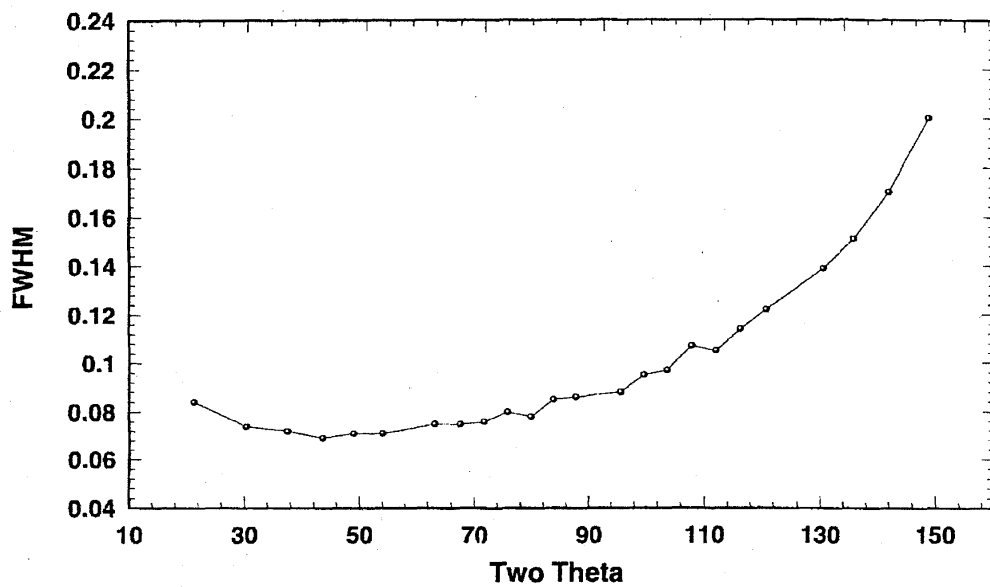


Figure 3 FWHM vs. two theta, on Siemens D500 with an IBM and PSD, determined with SRM 660, LaB₆.

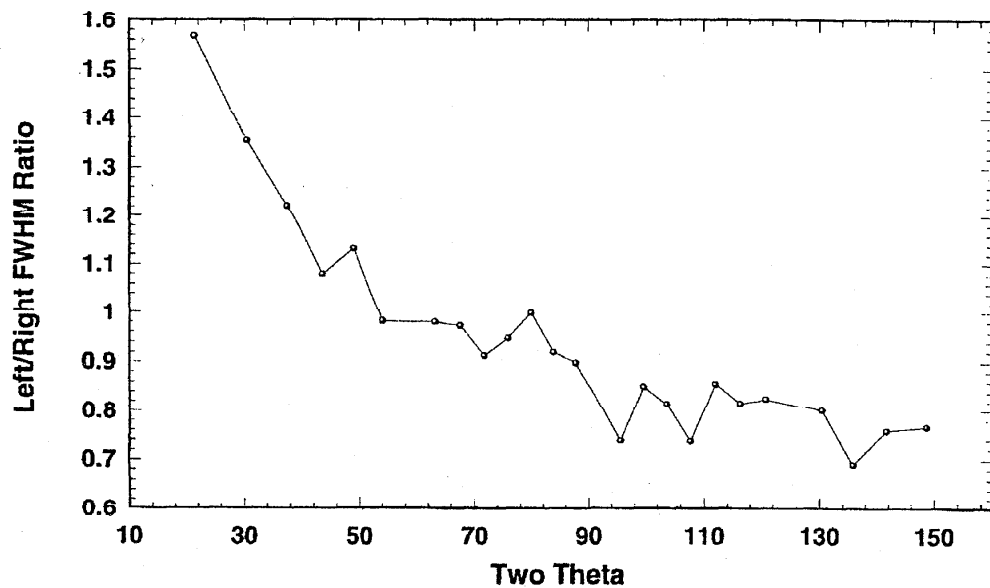


Figure 4 Peak width ratio, on Siemens D500 with an IBM and PSD, determined with SRM 660, LaB₆.

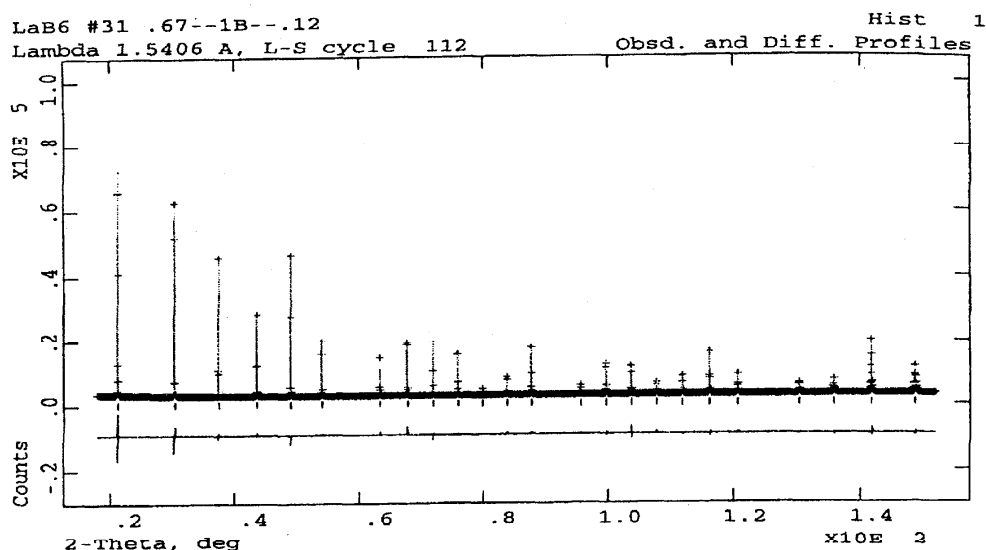


Figure 5 Rietveld analysis of NIST SRM 660, LaB₆.

resent the error associated with the fitting operation itself. However, experience has shown that these ESDs often underestimate a realistic assessment of a true standard deviation. The typical error bar computed from the ESDs associated with the FWHM values of Fig. 3 is smaller than the data point markers. There are several components contributing to the ESDs that are not accounted for in the profile model. Systematic errors, such as oscillatory errors in the indicated 2θ angle, which affect the data in a manner that includes multiple data points, are not accounted for in the reported ESDs. A visual inspection of the data in Figs. 2 through 4 and sound judgment are appropriate for discerning global defects in diffractometer performance. Discontinuities and lack of smoothness, in excess of a reasonable statistical variation, are indicative of systematic mechanical or electrical problems, which would expand and negate the reported ESDs. The identification of such difficulties warrants an additional investigation of the equipment.

The factors that contribute to the form of these plots will not be discussed in detail. However, the primary factors affecting their form are the equatorial divergence, the axial divergence, and the choice of receiving slit, in conjunction with the dispersion of the CuK α emission spectrum (Cheary & Cline, 1995; Cheary, Cline, & Anast, 1997; Cheary & Coelho, 1998). Of course, the data of Fig. 2 are dependent on the correct setting of the diffractometer zero point. At low angle, equatorial and axial divergence serve to asymmetrically broaden the profiles towards low angle. Hence, at low 2θ angle, peak maxima are shifted toward low angle in Fig. 2, FWHM values are slightly increased in Fig. 3, and the left/right ratio is increased in Fig. 4. At high angles, dispersion effects predominate, leading to the $\tan\theta$ -dependent increase in FWHM with 2θ shown in Fig. 3. Also with increasing 2θ , axial divergence and, to a lesser extent, the asymmetric nature toward lower energy of the CuK α emission spectrum leads to the shift in peak maxima toward high angle of Fig. 2 and the reduction in left/right ratio with 2θ shown in Fig. 4. At higher resolution settings,

ered: (1) One cannot refine the zero point while refining the shift, *trns*, asymmetry, and lattice parameters due to correlation problems, and (2) with the use of a glass slit for alignment, the goniometer zero point is determined to an accuracy approaching 0.0025 degrees during the alignment procedure. It is most appropriate to refine parameters about which one knows the least, and fix those of which one is quite certain. Therefore, when data from a standard are being analyzed, a decision is made whether to refine the goniometer zero or the lattice parameters. The present family of line position SRMs is certified to an uncertainty of parts in 10^{-5} ; however, this figure is considered greater than the uncertainty that may be obtained from a Rietveld analysis. While future SRMs will show improvement in uncertainty to the parts in 10^{-6} range, we choose to refine the lattice parameters as the goniometer zero is known with higher certainty.

Thus, we use the shift, *trns*, and asymmetry terms to model the data in Fig. 2, while the refined lattice parameters are compared with the certified values as a check on the results. This strategy is followed despite the fact that the phenomena associated with the models for sample displacement and beam penetration are by no means wholly responsible for the form of the data shown in Fig. 2. Inspection of the output indicates that the $\cos \theta$ model for sample displacement and $\sin 2\theta$ model for beam penetration (attenuation of the incident beam by the sample) are effective in modeling the data of Fig. 2 to result in lattice parameters accurate to within the uncertainties associated with the present generation of line position SRMs. A positive value of shift and a negative value of *trns* are expected in order to model the data in Fig. 2.

Owing to the high symmetry and preferred crystallographic orientation of LaB_6 , the refinement of the polarization correction is less than stable and yields a value that does not correspond to the computed value of a Ge (111) IBM. Thus, we employ SRM 676 for a final check of instrument performance. The profile parameters obtained from the refinement of SRM 660 correspond to the IPF, and therefore these values are used as the "floor" for subsequent refinements. The terms GP and GU are the Gaussian terms for size and strain broadening, respectively, while LX and LY are the corresponding Lorentzian terms. GV and GW are considered instrumental terms and are not refined. Refinement of the data from SRM 676 included the polarization term POLA (using the type 1 polarization correction of the GSAS code) but not a term for preferred orientation. Refinement results are shown in Table 3. We note an acceptable refinement with a POLA term of 0.92, which is in good agreement with the calculated value of 0.88. The temperature factors are also within reason. The asymmetry of the profiles could be expected to increase with the reduction in X-ray beam attenuation exhibited by the alumina relative to the LaB_6 . However, refinement of the asymmetry terms will result in a minimal reduction in the residual error terms and a nearly insignificant change in *S/L* and *H/L*, but often leads to instability.

In the event that the model-based methods are not to be used for evaluation of the equipment and/or there is a lesser concern for the form of the IPF, analysis of data from SRM 1976 can be used for an overall check of the instrument. The IPF can be evaluated using profile fitting to generate plots analogous to Figs. 2 through 4. Instrument sensitivity can be evaluated by generating the ratios of the observed to the certified intensities for the reflections listed on the SRM 1976 certificate. These data are then plotted versus 2θ as shown in Fig. 6. Due to heterogeneity in the degree of texture displayed by SRM 1976, plots such as Fig. 6 should be considered in their totality and not in terms of individual points. If one wishes to discern trends in the data, a polynomial fit can be useful. The data in Fig. 6 indicate a difficulty throughout the 2θ range, which is particularly problematic at high angle. While the causes of variation in instrument sensitivity are not well understood,

Table 3 Results From Rietveld Refinement of Al₂O₃, SRM 676

```

SRM 676 5/1/96 .6--18--.67          GENLRS Version VMS6 14:05:03 15-JUL-98 Page 12

Powder data statistics              Fitted      all      Average
Bank NData Sum(w*d**2)  wRp      Rp      wRp      Rp      DWG Integral
Stage 1 PXC 1 13397 83888.      0.1132 0.0830 0.1132 0.0830 0.388 0.951
Powder totals 13397 83888.      0.1132 0.0830 0.1132 0.0830 0.388

No serial correlation in fit at 90% confidence for 1.949 < DWG < 2.051
Cycle 76 There were 13397 observations. Total before-cycle CHI**2 = 8.3868E+04

Reduced CHI**2 = 6.278 for 18 variables

Reflection data statistics
Histogram 1 Type PXC Nobs= 65 R(**2) = 0.8332

The value of the determinant is 0.1386*10.0**( -8)

Atom parameters for phase no. 1
frac      x      y      z      100*Uiso 100*U11 100*U22 100*U33 100*U12 100*U13 100*U23
AL ( 1) Values : 1.000 0.000000 0.000000 0.000000 0.352204 0.249
      Sigmas :      0.000024 0.007
      Shift/Std:      -0.01 0.01
AL(1) moved 0.00A sum(shift/s.e.d)**2 : 0.00

O ( 2) Values : 1.000 0.306182 0.000000 0.250000 0.138
      Sigmas :      0.000108 0.013
      Shift/Std:      -0.01 0.01
O(2) moved 0.00A sum(shift/s.e.d)**2 : 0.00

Maximum atom shift: 0.00
Atomic parameter sum(shift/error)**2 for phase 1 : 0.00
Calculated unit cell formula weight: 611.766, Density: 3.986gm/cm**3

Histogram scale factors:
Histogram: 1 PXC
Scale : 151.632
Sigmas : 0.514895
Shift/Std: 0.00
Histogram scale factor sum(shift/error)**2 : 0.00

Lattice parameters for powder data:
Phase 1
a      b      c      alpha      beta      gamma      volume
Value : 4.75925 4.75925 12.99191 90.000 90.000 120.000 254.848
Sigmas : 0.00001 0.00001 0.00004 0.000 0.000 0.000 0.001
Reciprocal metric tensor shift factor = 100%
Reciprocal metric tensor sum(shift/error)**2 : 0.00

Diffractometer coefficients for powder data:
Hist. : 1 PXC
Dif A/Pola : 0.92848 Sigmas : 0.00913
Shift/Std : 0.01
Dif. Cons. Sum(shift/error)**2 : 0.00

Profile coefficients for histogram no. 1 and for phase no. 1:
Coeff. : GU      GV      GW      GP      LX      LY      S/L      H/L      trns      shift
Value : 2.300E+00 -3.100E+00 5.400E+00 1.318E+00 3.523E+00 2.200E+00 2.200E-02 2.150E-02 -1.573E-01 -1.061E+00
Sigmas : 6.100E-02 3.481E-02 5.932E-02
Shift/Std: 0.06 0.00 -0.03 0.07 -0.06
Coeff. : stoe      ptoe      sfoe      L11      L22      L33      L12      L13      L23
Value : 0.000E+00 0.000E+00 0.000E+00 0.000E+00 0.000E+00 0.000E+00 0.000E+00 0.000E+00 0.000E+00
Sigmas :
Shift/Std:
Profile coef. sum(shift/error)**2 : 0.01

Background coefficients for histogram no. 1:
Param. : 1      2      3      4      5
Coeff. : 1.739663E+02 -4.741770E+00 1.344739E+02 1.613099E-01 4.942401E+02
Sigmas : 4.718977E+00 1.890388E-01 3.526291E+01 4.359727E-03 3.322536E+01
Shift/Std: 0.00 0.00 0.00 0.00 0.00
Background coef. sum(shift/error)**2 : 0.00

Final sum((shift/Std)**2) for cycle 76 is 0.04 Time was 4.24 Sec
    
```

Table 3 Results From Rietveld Refinement of Al₂O₃, SRM 676

SRM 676 5/1/96 .6--18--.67 GENLES Version VMS6 14:05:03 15-JUL-98 Page 12

```

Powder data statistics
  Bank Wdata Sum(w*d**2) wRp Rp wRp Rp DWd Integral
Matgm  1 PXC  1 13397 83888.  0.1132 0.0830 0.1132 0.0830 0.388 0.951
Powder totals  13397 83888.  0.1132 0.0830 0.1132 0.0830 0.388

No serial correlation in fit at 98% confidence for 1.949 < DWd < 2.051
Cycle 76 There were 13397 observations. Total before-cycle CHI**2 = 8.3888E+04

Reduced CHI**2 = 6.278 for 18 variables

Reflection data statistics
Histogram 1 Type PXC Nobs= 65 R(F**2) = 0.0332

The value of the determinant is 0.1386*10.0**( -8)

Atom parameters for phase no. 1
      frac      x      y      z  100*Uiso 100*U11 100*U22 100*U33 100*U12 100*U13 100*U23
AL  ( 1) Values : 1.000 0.000000 0.000000 0.352208 0.249
      Sigmas :      0.000024 0.007
      Shift/esd:      -0.01 0.01
AL(1) moved 0.00A sum(shift/esd)**2 : 0.00

O  ( 2) Values : 1.000 0.386182 0.000000 0.250000 0.138
      Sigmas :      0.000108 0.013
      Shift/esd:      -0.01 0.01
O(2) moved 0.00A sum(shift/esd)**2 : 0.00

Maximum atom shift: 0.00
Atomic parameter sum(shift/error)**2 for phase 1 : 0.00
Calculated unit cell formula weight: 611.766, density: 3.986g/cm**3

Histogram scale factors:
Histogram: 1 PXC
Scale : 151.632
Sigmas : 0.514895
Shift/esd: 0.00
Histogram scale factor sum(shift/error)**2 : 0.00

Lattice parameters for powder data:
Phase 1
      a      b      c      alpha      beta      gamma      volume
Value : 4.75925 4.75925 12.99191 90.000 90.000 120.000 254.848
Sigmas : 0.00001 0.00001 0.00004 0.000 0.000 0.000 0.001
Reciprocal metric tensor shift factor = 100%
Reciprocal metric tensor sum(shift/error)**2 : 0.03

Diffractometer coefficients for powder data:
Hist. : 1 PXC
Dif A/Pole: 0.92848 Sigmas : 0.00913
Shift/esd : 0.01
Dif. Cons. Sum(shift/error)**2 : 0.00

Profile coefficients for histogram no. 1 and for phase no. 1:
Coeff. : GV GV GV GV LX LY S/L H/L trns shift
Value : 2.300E+00 -3.100E+00 5.400E+00 1.338E+00 3.523E+00 2.200E+00 2.200E-02 2.150E-02 -1.573E-01 -1.061E+00
Sigmas :      6.100E-02 3.491E-02 5.932E-02 4.430E-02 3.113E-02
Shift/esd:      0.05 0.00 -0.03 0.07 -0.06
Coeff. : stec ptec sfec L11 L22 L33 L12 L13 L23
Value : 0.000E+00 0.000E+00 0.000E+00 0.000E+00 0.000E+00 0.000E+00 0.000E+00 0.000E+00 0.000E+00 0.000E+00
Sigmas :
Shift/esd:
Profile coef. sum(shift/error)**2 : 0.01

Background coefficients for histogram no. 1:
Param. : 1 2 3 4 5
Coeff. : 1.739663E+02 -4.741770E+00 1.344739E+02 1.613099E-01 4.942401E+02
Sigmas : 4.718977E+00 1.890388E-01 3.326291E+01 4.359727E-03 3.332536E+01
Shift/esd: 0.00 0.00 0.00 0.00 0.00
Background coef. sum(shift/error)**2 : 0.00

Final sum((shift/esd)**2) for cycle 76 is 0.04 Time was 4.34 Sec
    
```

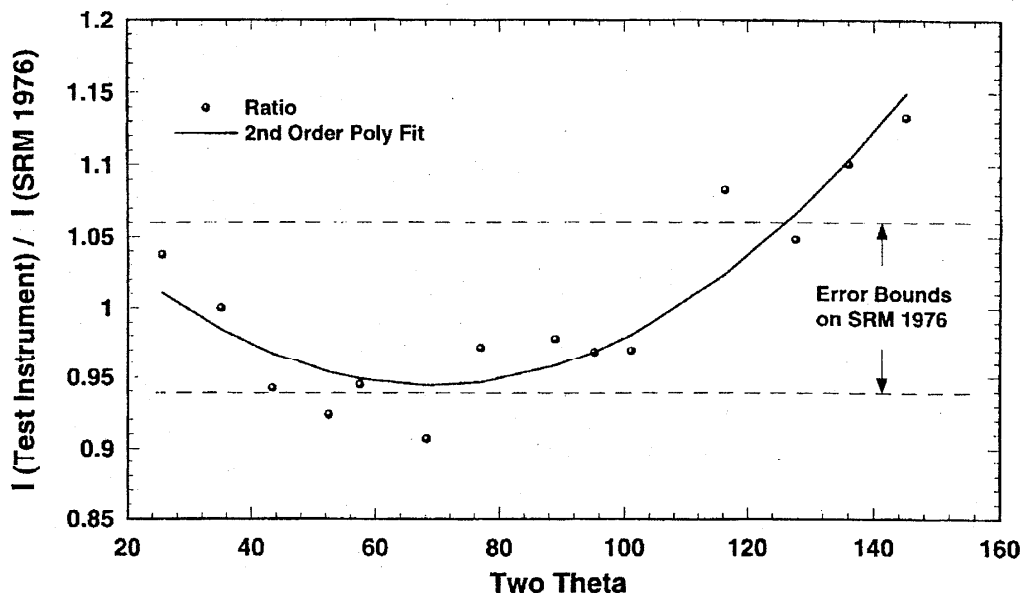


Figure 6 Evaluation of instrument response using SRM 1976, on a Siemens D500 with graphite post monochromator and scintillation detector.

we have observed large changes in sensitivity as the graphite post monochromator crystal is rotated through its rocking curve. Thus, while the intensity of a peak used to align the crystal may not be altered by an adjustment of the crystal 2θ angle, the instrument sensitivity could be affected, and the need for such an adjustment is indicated by the data in Fig. 6.

4. CONCLUSIONS

The para-focusing optics of divergent beam diffraction equipment, while providing a strong signal from weak X-ray sources, result in an instrument profile function that is sufficiently complex in origin that deficiencies in instrument performance are frequently overlooked. However, with proper instrument setup, the data collected from NIST SRMs will exhibit trends that can be modeled using either fundamental or analytical models to yield quantitative data on instrument performance. Both the Rietveld, or whole-pattern, and profile-fitting data analysis methods are required for a rigorous examination of instrument performance. The consideration of parameters obtained from profile fitting is necessary to discern defects that are confined to relatively small ranges of two-theta. The Rietveld method can be used to discern instrumental defects that span the entire two-theta range and also permits the instrument performance to be linked with independently determined crystal structure parameters. With the use of well-characterized and accurately aligned instrumentation, the credibility and range of useful information that can be obtained from a diffraction experiment are increased substantially.

REFERENCES

- Cagliotti, G., Paoletti, A., and Ricci, F. P. (1958). Nucl Instrumen, 3, 223-228.
 Cheary, R. W., and Cline, J. P. (1995). Adv. X-Ray Anal. 38, 75-82.